Visual Appearance of Matte Surfaces

Shree K. Nayar[1] **and Michael Oren**

Department of Computer Science

Columbia University

New York, NY 10027, U.S.A

[1]To whom correspondence should be addressed.

Abstract

All visual sensors, biological and artificial, are finite in resolution by necessity. This causes the effective reflectance of surfaces in a scene to vary with magnification. A reflectance model for matte surfaces is described that captures the effect of macroscopic surface undulations on image brightness. The model takes into account complex physical phenomena such as masking, shadowing and interreflections between points on the surface, and is shown to accurately predict the appearance of a wide range of natural surfaces. The implications of these results for human vision, machine vision, and computer graphics are demonstrated using both real and rendered images of three-dimensional objects. In particular, extreme surface roughness can cause objects to produce silhouette images devoid of shading, precluding visual perception of object shape.

Painters and sculptors are known to exploit their instinct for the interaction between light and materials[1, 2] to convey compelling shape cues to the observer [3]. Reflection of light by materials may be viewed as the first fundamental process in visual perception by human or machine. All reflectance mechanisms can be broadly classified into two categories: surface and body. In surface reflection, light rays are reflected at the interface between the surface medium and air. For very smooth surfaces, this results in specular or mirror-like appearance, the viewed surface producing a clear virtual image of its surroundings that is geometrically distorted when the surface is not planar [4]. As the surface gets rougher, the virtual image begins to blur, altering surface appearance from shiny to glossy, and even diffuse for high roughness values. Surface reflection is common, for instance, in metals.

In body reflection, incident light rays penetrate the surface and are scattered around due to reflections and refractions caused by inhomogeneities within the surface medium. Some of this light energy may be absorbed by the surface or transmitted through it. The remaining finds its way back to the interface to re-emerge as body reflection. The random nature of sub-surface scattering causes emerging light rays to be distributed in a wide range of directions, giving the surface a matte appearance. Body reflection plays a dominant role in materials like clay, plaster, concrete, and paper. In many natural materials however, both surface and body mechanisms coexist and together determine final visual appearance. Mathematical models for both reflection mechanisms, based on physical and geometrical optics, have been studied extensively.

For body reflection, numerous models have been suggested for the scattering process [5, 6, 7]. Among these, Lambert's law [5], proposed in 1760, remains the most widely used in visual psychophysics [8], computational vision [9], remote sensing [10], and computer graphics [11]. It predicts that the brightness, or radiance, L_r, of an ideal matte surface point is $\frac{\rho}{\pi}\cos\theta_i$, where ρ, the albedo or reflectivity, represents the fraction of the total incident light reflected by the surface, and θ_i is the incidence angle between the surface normal and the illumination direction. The popularity of Lambert's model can be attributed to its ability to predict with a fair degree of accuracy the appearance of a large spectrum of real-world materials. Another reason is undoubtedly its simple mathematical form, which lends itself to numerous interesting appearance properties; for theoreticians and practitioners alike, the use of Lambert's law is a temptation difficult to resist. Both reasons have led to its widespread use in understanding and emulating perception of important visual cues such as shading.

The most appealing aspect of Lambert's law is its prediction that the brightness of a scene point is independent of the observer's viewpoint. This in turn can be exploited to establish that a scene point illuminated by several light sources can be viewed as illuminated by a single source whose intensity and direction are given simply by the centroid of all the sources. Furthermore, the surface normal and albedo of a scene point can be uniquely determined from its brightness values measured using three known illuminants [12]. The simplicity of Lambert's law permits even the analysis of complex high-order phenomena such as interreflections [13, 14], the bouncing of light rays between mutually visible points on a concave surface. In the presence of interreflections, a surface continues to behave exactly like a Lambertian one without interreflections but with a different set of normals and albedo values [15].

Alas, our visual world limits the scope of Lambert's model. While it does well in describing sub-surface scattering in a large variety of materials, it fails to describe the ubiquitous interplay between surface undulations and image resolution (Figure 1). Visual processing by humans and machines must rely on finite-resolution sensors. Photoreceptors of the retina and pixels in a video camera are both by necessity finite-area detectors; light intensity can be recorded only by counting photons collected in buckets of measurable size. This finite resolution, along with the optical point spread [16] inherent to any imaging system, cause each receptor to receive light not from a single point but rather from a surface area in the scene, this area increasing as the square of the distance of the surface from the eye or the camera (Figure 1b). Often, substantial macroscopic ($\gg$ wavelength of the incident light) surface roughness is projected onto a single detector, which in turn produces an aggregate brightness value. Whereas Lambert's law may hold well when observing a single planar facet (near sight), a collection of such facets with different orientations (far sight) is guaranteed to violate Lambert's law. The primary reason is the variation in foreshortened facet areas under motion of the observer (Figure 2a). Analysis of this phenomenon has a long history and can be traced back almost a century. Past work has resulted in empirical models [17, 18] designed to fit experimental data as well as theoretical results derived from first principles [19, 20, 21]. Much of this work was motivated by the non-Lambertian reflectance of the moon [22, 23, 24]. Unfortunately, these models are severely limited in scope either by the specific surface geometry assumed or by their inability to predict brightness for the entire hemisphere of source and sensor directions.

A new reflectance model has been developed that describes the relation between macroscopic surface roughness and sensor resolution. The surface patch imaged by each sensor detector is modeled as a collection of numerous long symmetric V-shaped cavities (Figure 2b); each cavity has two planar Lambertian facets with opposing normals, facet normals are free to deviate from the mean surface normal, and all facets on the surface have the same albedo ρ. It is assumed that the V-cavities are uniformly distributed in orientation ϕ_a (azimuth angle) on the surface plane, whereas facet tilt θ_a (polar angle) is normally distributed with zero mean and standard deviation σ, the latter serving as a roughness parameter[1]. This isotropic surface model has been previously used to study surface reflection from rough surfaces [25], and is invoked here to achieve mathematical tractability[2]. When $\sigma = 0$, all facet normals align with the mean surface normal, producing a planar patch that obeys Lambert's law. However, as σ increases, the V-cavities get deeper on the average, and the deviation from Lambert's model increases.

[1]Roughness, as defined here, is a purely macroscopic property. It is not indicative of the microscopic structure of the surface with is assumed to cause the surface to be locally Lambertian.

[2]Natural surfaces clearly profess a wide spectrum of macroscopic surface geometries. For deriving reflectance, a specific surface model must be assumed. In the past, several surface models [19, 20] have been found to be difficult to manipulate during reflectance model derivation. In the context of body reflection, radiance in the direction of the observer must be evaluated as an integral over all visible points on the surface patch projecting onto a single sensor detector. Since integration has the effect of weighted averaging, it turns out that several surface models are capable of capturing the primary reflectance characteristics of the surface. The V-cavity model [21] was chosen as it facilitates the analysis of pertinent radiometric and geometric phenomena and hence results in a reflectance model that performs fairly well for a large variety of real surfaces.

The reflection model captures not only the foreshortening of individual facets (Figure 2a), but also masking, shadowing, and interreflections (up to two bounces) between adjacent facets [26]. The brightness of a surface patch is expressed as the integral of facet brightness over all facet normals. This integral is cumbersome to evaluate and must be broken into components representing facets that are masked, shadowed, masked and shadowed, and neither masked nor shadowed. The complexity of the integral is easily seen by imagining the different masking and shadowing conditions that arise as a single V-cavity is rotated in the surface plane. A solution to the integral was arrived at by first deriving a basis function for each component of the integral, and then finding coefficients for the bases through extensive numerical simulations [26]. The accuracy of the model was verified by matching model predictions with reflectance measurements from natural surfaces, such as, plaster, sand, and clay (Figure 3). In all cases, predicted and measured data were found to be in strong agreement. A systematic increase in brightness is observed as the sensor moves towards the illuminant; this backscattering is in contrast to Lambertian behavior where brightness is constant and independent of sensor direction, and also in contrast to surface reflection where a peak in brightness is expected in the vicinity of the specular direction [25]. For applications where simplicity is desired over high precision, approximations were made to arrive at this qualitative model:

$$
\begin{aligned}
L(\theta_r, \theta_i, \phi_r - \phi_i; \rho, \sigma) &= \frac{\rho}{\pi} E_0 \cos\theta_i (A + B\,Max\Big[0, \cos(\phi_r - \phi_i)\Big] \sin\alpha \tan\beta)\,, \qquad (1) \\
A &= 1.0 - 0.5 \frac{\sigma^2}{\sigma^2 + 0.33}\,, \\
B &= 0.45 \frac{\sigma^2}{\sigma^2 + 0.09}\,,
\end{aligned}
$$

where E_0 is the intensity of the source, (θ_r, ϕ_r) and (θ_i, ϕ_i) are the observer and illuminant directions in a coordinate frame with its z-axis aligned with the surface normal, and $\alpha = Max(\theta_r, \theta_i)$ and $\beta = Min(\theta_r, \theta_i)$.

The developed model may be viewed as a generalization of Lambert's law, which is simply an extreme case with $\sigma = 0$. The model has direct implications for shape recovery in machine vision [26] and for realistic rendering in computer graphics [28]. Further, it provides a firm basis for studying visual perception of three-dimensional objects. To illustrate this, several objects were constructed from materials such as porcelain and stoneware, and their digital images shown to closely match synthetic ones rendered using the model (Figure 4). Both real and rendered shadings are seen to vary synchronously, and significantly, with macroscopic roughness.

These experiments have led to a curious observation: The model predicts that for very high macroscopic roughness, when the observer and the illuminant are close to one another, all surface normals will generate approximately the same brightness. This implies that, a three-dimensional object, irrespective of its shape, will produce nothing more than a silhouette with constant intensity within. In the case of polyhedra, edges between adjacent faces will no longer be discernible (Figure 4a), and smoothly curved objects will be devoid of shading (Figure 1a). This visual ambiguity may be viewed as a perceptual singularity in which interpretation of the three-dimensional shape of an object from its image is impossible for both humans and machines. This phenomenon offers a plausible explanation for the flat-disc appearance of the full moon (Figure 4e).

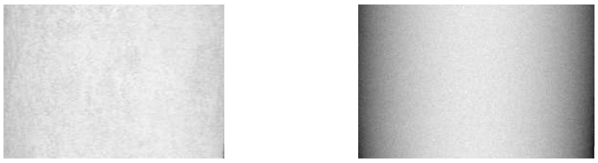

(a)

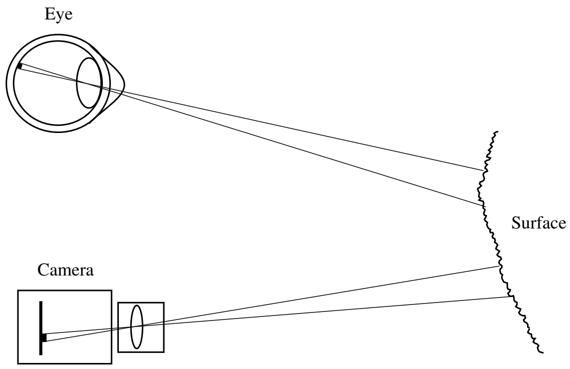

(b)

Figure 1: (a) Digital images of two surface patches illuminated from the same direction. The strong shading of the right patch leads the observer to perceive a cylindrical surface with a vertical axis. In contrast, the left patch has fairly uniform brightness and the lack of shading seems to suggest a planar surface. The actual shapes of the surfaces are identical. Both patches are clipped from images (512x480 pixels) of cylindrical vases. On the left is a real clay vase with very rough exterior that gives it a flat appearance. The right vase has identical shape but is rendered using Lambert's model [5] for body reflection. Lambert's law predicts strong shading and drives brightness at the occluding boundaries to zero. While it predicts the reflectance of several natural surfaces with adequate accuracy, it fails to capture the interplay between macroscopic surface roughness and sensor resolution. (b) Retina of the human eye [16] and solid-state sensors in video cameras have finite-size receptors that aggregate brightness from areas rather than points in the scene. The area projected onto a single receptor increases as square of surface distance from the sensor. In a typical CCD camera used with a 25 mm lens, each pixel images a foreshortened area of 9 mm^2 at a distance of 5 m, or 144 mm^2 at 20 m. Clearly, large amounts of macroscopic undulations can project onto a single pixel.

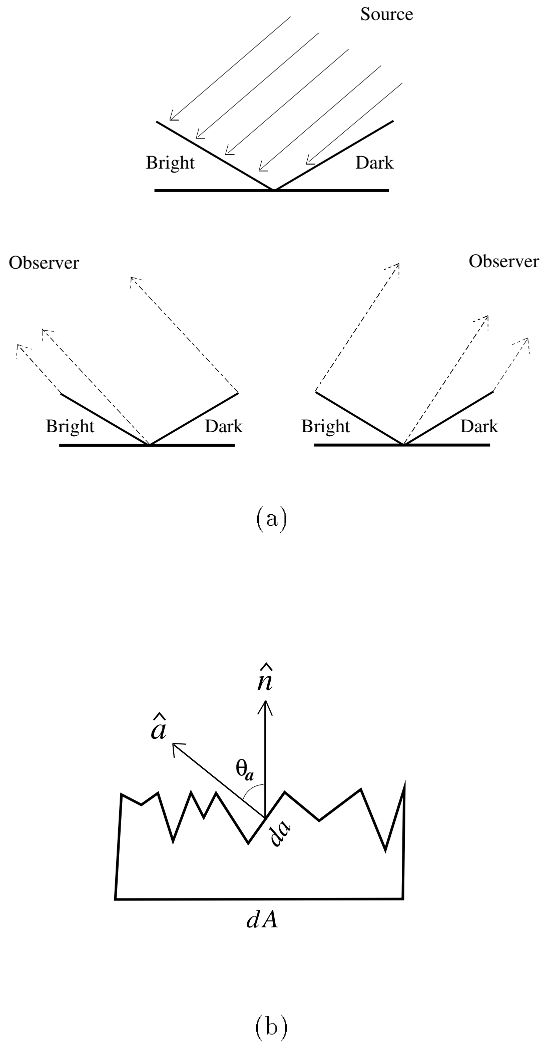

Figure 2: (a) A single V-cavity used to illustrate why a collection of Lambertian facets with different orientations does not obey Lambert's law. When the cavity is illuminated from the right, the smaller incidence angle for the left facet makes it brighter than the right one. For an observer on the left, the foreshortening of the left facet is greater than of the right one and a larger fraction of the cavity is dark. As the observer moves right, towards the illuminant, the fraction of the brighter area increases, causing the aggregate brightness of the V-cavity to rise. (b) A reflectance function is derived by modeling a surface patch as a collection of V-cavities ($da \ll dA$) with different facet normals ($\hat{a}$).

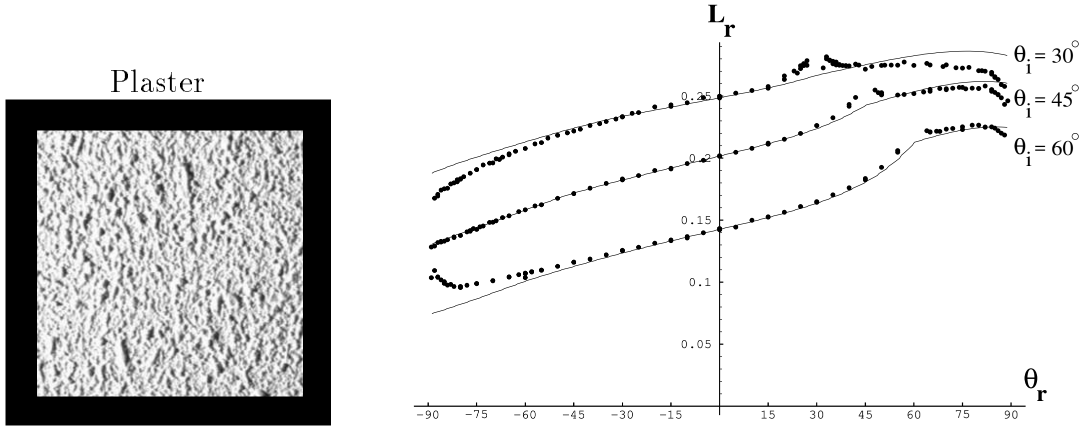

Figure 3: Measured reflectance (dots) is compared with reflectance predicted by the model (solid lines) for plaster. Surface radiance L_r, computed as an average over the entire surface patch, is plotted as a function of sensor direction θ_r for three angles of incidence θ_i. Albedo ρ and roughness σ were selected to achieve the best fit. In these measurements, the source direction, sensor direction, and the mean surface normal are coplanar ($\phi_i = \phi_r = 0$). Surface brightness increases as the sensor approaches source direction, violating Lambert's law that predicts brightness to be independent of viewing direction. This brightness increase is also in contrast to surface reflection mechanisms that produce peaks around the specular direction. In these and other experiments [26], the proposed model is found to be in strong agreement with measured data. The narrow peak observed in the source direction is attributed to the opposition effect [27]. This phenomenon is of relatively less import to visual perception as it requires the observer and the source to be within a few degrees from each other, a situation difficult to emulate in practice without either one obstructing the other. The scope of the proposed model is broadened by combining it [26] with previously suggested ones for surface reflection [25] that are based on similar roughness assumptions. Validity of such a combined model was verified using samples such as sand, cloth, foam, sandpaper, and wood.

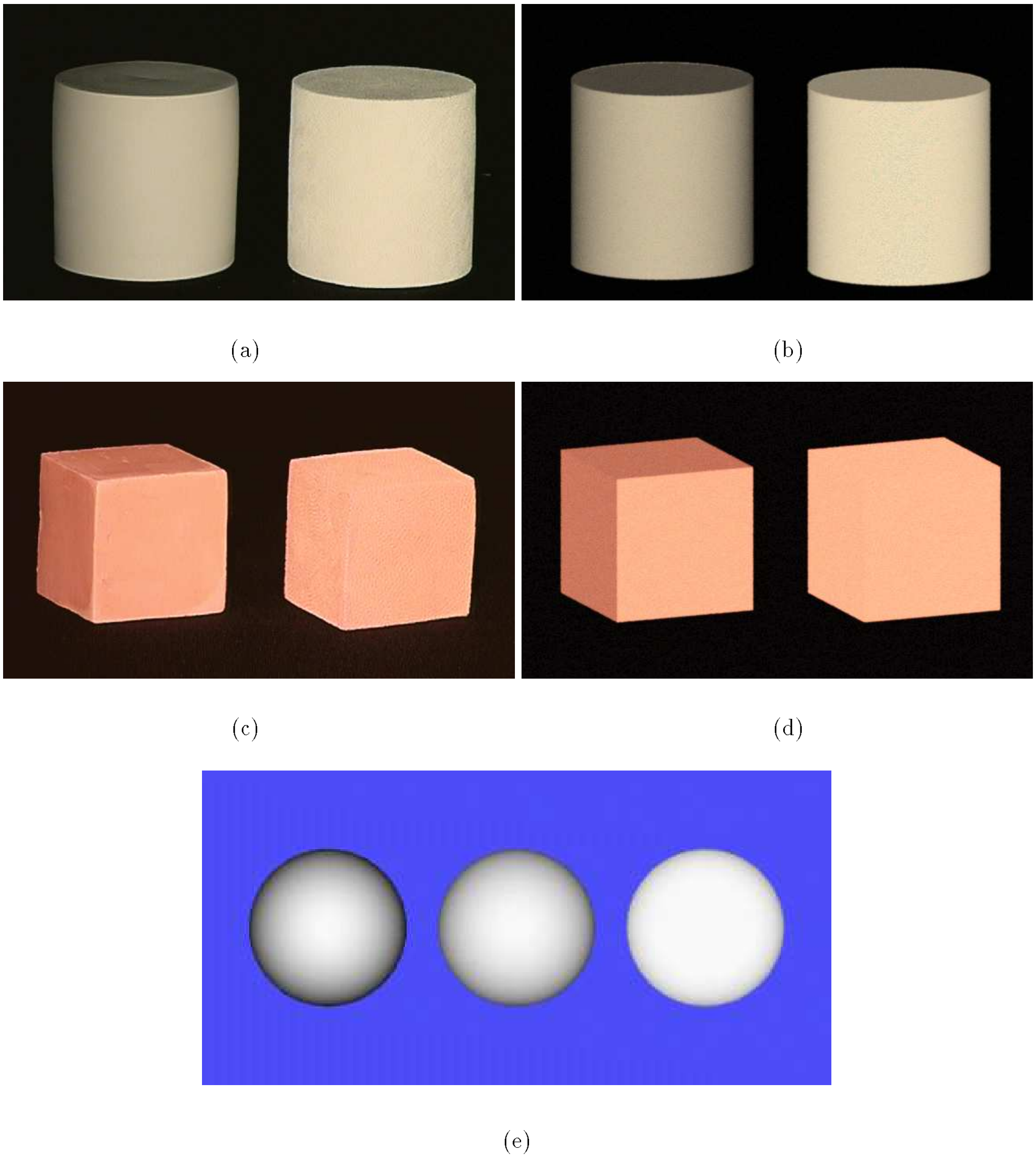

Figure 4: (a) Video camera image of two cylinders made from exactly the same material (porcelain) and illuminated from approximately 10° above the camera. The right vase is much rougher than the left one resulting in flatter appearance. (b) Synthetic image of cylinders with similar dimensions, rendered using the theoretical model (left: $\sigma = 5°$, right: $\sigma = 35°$). (c) Camera image of two cubes made from stoneware, illuminated from approximately 18° to the left of the camera. (d) Synthetic image of cubes (left: $\sigma = 7°$, right: $\sigma = 40°$). In both real and synthetic images, low macroscopic roughness of the left cube results in nearly Lambertian appearance, whereas very high roughness of the right cube causes all three faces to produce almost the same brightness with clear edges no longer visible. The model and experiments suggest that for very high macroscopic roughness, when source and sensor directions are close to one another, all surface normals generate the same image brightness. Alternately, any object, irrespective of its three-dimensional shape, produces just a silhouette making it impossible to perceive shape. (e) Spheres illuminated and viewed from the same direction. As roughness increases (left to right: $\sigma = 0°$; $\sigma = 15°$; $\sigma = 40°$;) shading becomes flatter. For extreme roughness (right), the sphere appears like a flat disc, as observed in the case of the full moon.

References

[1] L. da Vinci, *Treatise on Painting*, A. P. McMahon, Trns. (University Press, Princeton, 1959).

[2] H. W. Janson, *History of Art* (Prentice Hall and H. N. Abrams, New York, 1991).

[3] D. S. Strong, *Leonardo on the eye* (Garland Publications, New York, 1979).

[4] B. Geist, *Brancusi: the sculpture and drawings* (H. N. Abrams, New York, 1975).

[5] J. H. Lambert, *Eberhard Klett* (1760).

[6] P. Kubelka and F. Munk, *Z. tech. Physik*, **12**, 593 (1931).

[7] S. Chandrasekhar, *Radiative Transfer* (Dover Publications, 1960).

[8] V. S. Ramachandran, *Nature*, **331**, 6152 (1988).

[9] B. K. P. Horn and M. J. Brooks, Eds. *Shape from Shading* (MIT Press, 1989).

[10] J. A. Smith, T. L. Lin, K. J. Ranson, *Photogrammetric Engineering and Remote Sensing* (1980).

[11] M. F. Cohen and J. R. Wallace, *Radiosity and Realistic Image Synthesis* (Academic Press Professional, Boston, 1993).

[12] R. J. Woodham, *Optical Engineering*, **19**, 1 (1980).

[13] J. J. Koenderink and A. J. van Doorn, *Journal of the Optical Society of America*, **73**, 6 (1983).

[14] D. Forsyth and A. Zisserman, in *Proc. IEEE Conf. on Computer Vision and Pattern Recognition* (1989).

[15] S. K. Nayar, K. Ikeuchi, T. Kanade, *International Journal of Computer Vision*, **6**, 3 (1991).

[16] G. Westheimer, in *Medical Physiology,* V. B. Mountcastle, Ed. (C. V. Mosby Company, St. Louis, ed. 14, 1980), vol. 1, chap. 16.

[17] E. Opik, *Publications de L'Observatorie Astronomical de L'Universite de Tartu*, **26**, 1 (1924).

[18] M. Minnaert, *Astrophysical Journal*, **93** (1941).

[19] B. G. Smith, *Journal of Geophysical Research*, **72**, 16 (1967).

[20] D. Buhl, W. J. Welch, D. G. Rea, *Journal of Geophysical Research*, **73**, 16 (1968).

[21] R. G. Hering and T. F. Smith, *AIAA Prog. in Astronautics and Aeronautics*, **23** (1970).

[22] N. S. Orlova, *Astron. Z.* (1956).

[23] R. Siegel and J. R. Howell, *Thermal Radiation Heat Transfer* (Hemisphere Publishing Corporation, 1956).

[24] B. W. Hapke and H. van Horn, *Journal of Geophysical Research*, **68**, 15 (1963).

[25] K. E. Torrance and E. Sparrow, *Journal of the Optical Society of America*, **57** (1967).

[26] M. Oren and S. K. Nayar, *International Journal of Computer Vision*, in press (1995).

[27] B. W. Hapke, R. M. Nelson, W. D. Smythe, *Science*, **260**, 23 (1993).

[28] M. Oren and S. K. Nayar, in *Proc. ACM SIGGRAPH* (1994).

Acknowledgements

This work was supported by an ARPA grant and a David and Lucile Packard Fellowship to SKN and an IBM Graduate Fellowship to MO. We thank V. Nalwa of Bell Laboratories and A. Aggarwal, M. Lai and S. Baker of Columbia University for valuable suggestions. Thanks to S. Nene of Columbia University for assistance with the images.